Cell

Cyclin F-Mediated Degradation of Ribonucleotide Reductase M2 Controls Genome Integrity and DNA Repair

Vincenzo D'Angiolella,[1] Valerio Donato,[1] Frances M. Forrester,[1] Yeon-Tae Jeong,[1] Claudia Pellacani,[1] Yasusei Kudo,[1,2] Anita Saraf,[3] Laurence Florens,[3] Michael P. Washburn,[3,4] and Michele Pagano[1,5,*]

[1]Department of Pathology, NYU Cancer Institute, New York University School of Medicine, 522 First Avenue, SRB 1107, New York, NY 10016, USA

[2]Department of Oral Molecular Pathology, Institute of Health Biosciences, The University of Tokushima Graduate School, Tokushima 770-8501, Japan

[3]The Stowers Institute for Medical Research, 1000 East 50th Street, Kansas City, MO 64110, USA

[4]Department of Pathology and Laboratory Medicine, The University of Kansas Medical Center, 3901 Rainbow Boulevard, Kansas City, KS 66160, USA

[5]Howard Hughes Medical Institute

*Correspondence: michele.pagano@nyumc.org

DOI 10.1016/j.cell.2012.03.043

SUMMARY

F-box proteins are the substrate binding subunits of SCF (Skp1-Cul1-F-box protein) ubiquitin ligase complexes. Using affinity purifications and mass spectrometry, we identified RRM2 (the ribonucleotide reductase family member 2) as an interactor of the F-box protein cyclin F. Ribonucleotide reductase (RNR) catalyzes the conversion of ribonucleotides to deoxyribonucleotides (dNTPs), which are necessary for both replicative and repair DNA synthesis. We found that, during G2, following CDK-mediated phosphorylation of Thr33, RRM2 is degraded via $SCF^{cyclin\ F}$ to maintain balanced dNTP pools and genome stability. After DNA damage, cyclin F is downregulated in an ATR-dependent manner to allow accumulation of RRM2. Defective elimination of cyclin F delays DNA repair and sensitizes cells to DNA damage, a phenotype that is reverted by expressing a nondegradable RRM2 mutant. In summary, we have identified a biochemical pathway that controls the abundance of dNTPs and ensures efficient DNA repair in response to genotoxic stress.

INTRODUCTION

The ubiquitin-proteasome system allows the precise temporal and spatial regulation of a large variety of regulatory proteins. This tight control is accomplished through the specific, targeted degradation of proteins via ubiquitin ligases. The Skp1-Cul1-F-box protein (SCF) complexes are the canonical multisubunit E3 ubiquitin ligases and assemble by using Cul1 as a core scaffold (Cardozo and Pagano, 2004; Petroski and Deshaies, 2005). The small RING protein Rbx1 and an ubiquitin conjugating enzyme (UBC) are recruited via the C terminus of Cul1. The Cul1 N terminus, instead, binds the bridging factor Skp1 and a variable F-box protein, which determines substrate specificity. Each F-box protein can target multiple substrates, allowing the core SCF scaffold, by using different F-box proteins, to target hundreds of substrates for degradation (Jin et al., 2004). Of the 69 human F-box proteins, only a minority have established functions (Skaar et al., 2009).

Cyclin F (also known as Fbxo1) is the founding member of the F-box protein family and is essential for mouse development (Bai et al., 1996; Tetzlaff et al., 2004). In addition to an F-box domain, cyclin F contains a cyclin box domain, but, in contrast to typical cyclins, it does not bind or activate any cyclin-dependent kinases (CDKs) (Bai et al., 1996; D'Angiolella et al., 2010; Fung et al., 2002; Tetzlaff et al., 2004). However, like other cyclins, cyclin F protein levels oscillate during the cell division cycle, peaking in G2.

Cyclin F localizes to both the centrosomes and the nucleus (D'Angiolella et al., 2010). During G2, centrosomal cyclin F targets CP110 for proteasome-mediated degradation to limit centrosome duplication to once per cell cycle (D'Angiolella et al., 2010). Additionally, cyclin F promotes the degradation of NuSAP1, a protein involved in mitotic spindle organization (Emanuele et al., 2011). The biological function of nuclear cyclin F remains unknown.

Ribonucleotide reductase (RNR) is a well-studied enzyme composed of two identical, large subunits (called RRM1, RNR1, RR1, or R1) and two identical small subunits (called RRM2, RNR2, RR2, or R2) (Nordlund and Reichard, 2006). A functional catalytic site is constituted when two RRM2 (*r*ibonucleotide *r*eductase family *m*ember 2) subunits are bound to two RRM1 (*r*ibonucleotide *r*eductase family *m*ember 1) subunits. RNR catalyzes the conversion of ribonucleotides to deoxyribonucleotides (dNTPs), which are used in the synthesis of DNA during replication and repair (Nordlund and Reichard, 2006). Because of this fundamental function, RNR is among

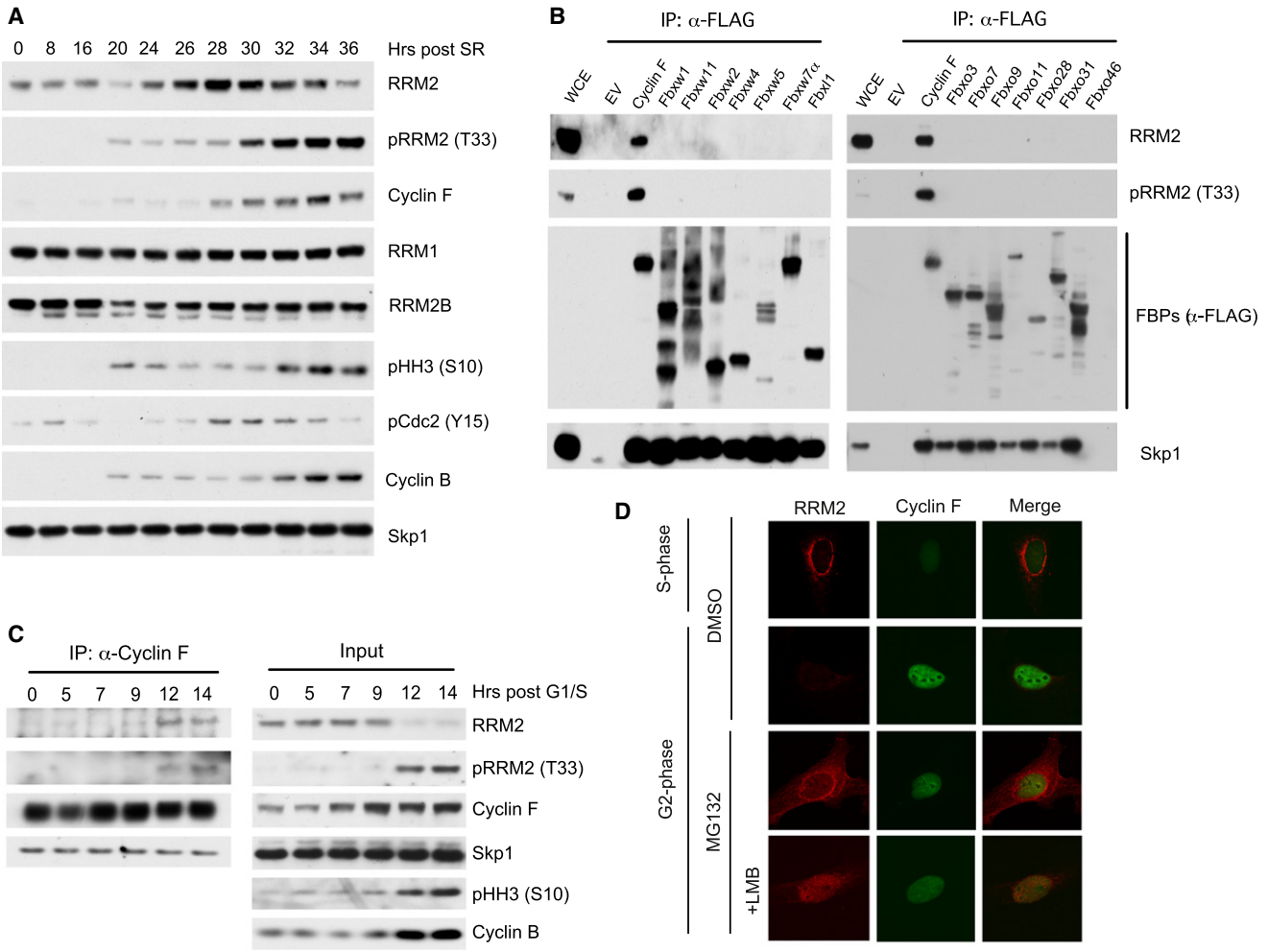

Figure 1. Cyclin F and RRM2 Physically Interact and Colocalize to the Nucleus in G2

(A) RPE1-hTERT cells were synchronized in G0/G1 by 72 hr of serum starvation before release into fresh medium containing serum. Cells were collected at the indicated time points after serum readdition (SR), lysed, and immunoblotted as indicated.

(B) HEK-293T cells were transfected with an empty vector (EV) or the indicated FLAG-tagged F-box protein constructs (FBPs). Whole-cell extracts were immunoprecipitated (IP) with anti-FLAG resin, and immunoprecipitates were immunoblotted as indicated.

(C) HeLa cells were synchronized at G1/S by using a double-thymidine block before release into fresh medium. Cell lysates were generated at the indicated time points, immunoprecipitated with an antibody to cyclin F, and immunoblotted as indicated. Ten percent of the material used for immunoprecipitation (input) is shown on the right panels.

(D) U-2OS cells were synchronized at G1/S by using a double-thymidine block before release into fresh medium. Cells were fixed at 5 hr (S phase) and 9 hr (G2 phase) after release from the block and stained with an antibody to cyclin F (green) or RRM2 (red). Where indicated, cells where pretreated for 2 hr with Leptomycin B (LMB) before fixation. Confocal microscopy was used to visualize stained cells.

See also Table S1.

the most well-conserved (from prokaryotes to eukaryotes) and highly-regulated enzymes. Indeed, dNTP pool increases or imbalances produce a hypermutator phenotype (Hu and Chang, 2007; Kunz et al., 1998), and decreased dNTP levels interfere with proper DNA replication and repair (Nordlund and Reichard, 2006).

RNR activity needs to be coordinated with cell-cycle progression to preserve the fine balance between dNTP production and DNA replication. RRM1 levels are constant throughout the cell cycle and are always in excess of the level of RRM2, which fluctuates during the cell cycle (Chabes and Thelander, 2000 and Figure 1A). Therefore, the cell-cycle-dependent activity of RNR is regulated by RRM2 levels. The G1/S induction of RRM2 transcription is dependent on the transcription factor E2F1 (Chabes et al., 2004; DeGregori et al., 1995), and, to prevent RRM2 accumulation in G1, RRM2 levels are also kept in check by the APC/C^{Cdh1} ubiquitin ligase (Chabes et al., 2003b). Notably, how RRM2 is degraded in the G2 phase of the cell cycle remains unknown.

Although RNR is a cytoplasmic enzyme, in response to genotoxic stress, it translocates from the cytoplasm to the nucleus to ensure the local availability of dNTPs at DNA damage sites for

DNA repair (Niida et al., 2010; Xu et al., 2008; Xue et al., 2003; Zhang et al., 2009).

Here, we report the identification of RRM2 as a nuclear substrate of the $SCF^{cyclin\ F}$ ubiquitin ligase and describe the role of this interaction in ensuring genome stability and efficient DNA repair synthesis.

RESULTS

During G2, Cyclin F Interacts with RRM2 in the Nucleus

To identify substrates of the $SCF^{cyclin\ F}$ ubiquitin ligase, FLAG-HA-tagged cyclin F was transiently expressed in either HeLa or HEK293T cells and immunopurified for analysis by Multidimensional Protein Identification Technology (MudPIT) (D'Angiolella et al., 2010; Florens and Washburn, 2006). MudPIT revealed the presence of peptides corresponding to Skp1 and Cul1, as well as peptides derived from RRM2 (Table S1). Combining both analyses, 23 total spectra, corresponding to five unique RRM2 peptides, were identified. In two additional experiments, we immunopurified cyclin F(1-270), a cyclin F mutant lacking the cyclin box, and although Skp1 and Cul1 still coimmunoprecipitated with cyclin F(1-270), binding to RRM2 was not detected (Table S1).

To investigate whether the binding between RRM2 and cyclin F is specific, we screened a panel of human F-box proteins. Fifteen FLAG-tagged F-box proteins were expressed in HEK293T cells (with the proteasome inhibitor MG132 added for 6 hr prior to harvesting) and immunoprecipitated to evaluate their interaction with RRM2. We found that the only F-box protein able to coimmunoprecipitate endogenous RRM2 was cyclin F (Figure 1B). Through the use of synchronized HeLa cells (monitored by immunoblotting for cell-cycle markers and flow cytometry), the interaction between endogenous cyclin F and endogenous RRM2 was observed exclusively in G2 and early M (Figure 1C), when the levels of cyclin F increase and RRM2 levels are drastically reduced (Figures 1A and 1C).

Because cyclin F localizes to both the nucleus and centrosomes (D'Angiolella et al., 2010) and RRM2 is largely cytoplasmic (Nordlund and Reichard, 2006), we asked where and when the two proteins could colocalize. Synchronized U-2OS cells were costained with antibodies to RRM2 and cyclin F. As expected, cyclin F was nuclear, whereas RRM2 was localized to the cytoplasm in S phase cells and virtually absent in G2 cells (Figure 1D). However, treatment of G2 cells with MG132, a proteasome inhibitor, induced the accumulation of RRM2 in both the nucleus and cytoplasm, as shown by confocal immunofluorescence (Figure 1D). We also observed that, upon a brief treatment of G2 cells with MG132 and the CRM1/exportin1 inhibitor Leptomycin B (LMB), RRM2 accumulated mostly in the nucleus (Figure 1D, bottom panels). These results suggest that during G2, RRM2 enters the nucleus to interact with and be degraded via cyclin F, consistent with coimmunoprecipitation experiments (Figure 1C).

We also mapped the RRM2 binding domain on cyclin F by using a series of deletion mutants. A truncated version of cyclin F that lacks the cyclin box domain and cyclin F mutated in its hydrophobic patch domain [cyclin F(M309A)] failed to bind RRM2 (Figures 2A and S1A–S1B, available online), similar to results obtained with CP110 (D'Angiolella et al., 2010). However, cyclin F(1-549), which retains the cyclin box domain but does not localize to the nucleus (Figure S1C), was unable to bind RRM2 (Figures S1A–S1B), although this mutant still interacted with CP110 (D'Angiolella et al., 2010), further confirming that the cyclin F and RRM2 interact in the nucleus.

A CY Motif and Thr33 Are Required for RRM2 Binding to Cyclin F

Subsequently, we mapped the cyclin F binding motif in RRM2. A series of binding experiments, which used multiple RRM2 deletion mutants, narrowed the binding motif to a region of RRM2 located between amino acids 40–65 (Figures S2A–S2B). This region contains two putative CY motifs (RxL and RxI) (Figure 2B), which are established cyclin binding domains (Schulman et al., 1998). A mutant in the second motif [RRM2(RxI/AxA)] failed to coimmunoprecipitate endogenous cyclin F (Figure 2C), indicating that this CY motif, located at residues 49–51 of RRM2, mediates binding to cyclin F. In parallel, we also performed Ala scanning mutagenesis of the region encompassing amino acids 22–40 and found that, in addition to the CY motif, Thr33 is also necessary for an efficient binding to cyclin F (Figures 2B and 2C and S2C). Thr33 was previously identified as a phosphorylated site in proteomic screens (Daub et al., 2008; Mayya et al., 2009), therefore, we generated a phospho-specific antibody against a peptide corresponding to amino acids 35–50 of human RRM2 with Thr33 phosphorylated. This antibody recognized wild-type RRM2 but not RRM2(T33A), a mutant in which Thr33 was mutated to Ala (Figures 2C and S2C). Using this antibody, we found that cyclin F coimmunoprecipitated the phosphorylated form of endogenous RRM2 (Figures 1B and 1C). Significantly, RRM2 was phosphorylated on Thr33 predominantly in G2 and M (as indicated by the increase in cyclin B levels and Histone H3 phosphorylation on Ser10), when the levels of total RRM2 decrease and RRM2 interacts with cyclin F (Figures 1A and 1C).

Thr33 in RRM2 Is Phosphorylated by CDKs to Promote Binding to Cyclin F

The presence of a Pro at position 34 suggested that a Pro-directed kinase phosphorylates Thr33, and the phosphorylation of this residue in G2 and early M suggested that this kinase could be a CDK. In support of this hypothesis, we found that three different CDK inhibitors (NU6102, Roscovitine, and Alsterpaullone) reduced RRM2 phosphorylation on Thr33, whereas SB203580 (a p38 inhibitor), U0126 (a MEK inhibitor), DMAT (a CKII inhibitor), and LY293646 (a DNA-PK inhibitor) had no effect (Figure 2D). Moreover, both Cdk1-cyclin B and Cdk2-cyclin A, but not Plk1 (another G2/M kinase), phosphorylated RRM2 on Thr33 in vitro, as shown by immunoblotting with the phospho-specific antibody (Figure 2E and data not shown). Importantly, CDK-dependent phosphorylation of RRM2 was necessary for its in vitro binding to cyclin F (Figure 2F).

Both Thr33 and the CY motif of RRM2 are highly conserved across species (Figure S2D), and both are necessary, but not sufficient, for a stable binding of RRM2 to cyclin F. RRM2(T33A), which contains an intact CY motif, did not efficiently bind cyclin F in vivo or in vitro (Figures 2C, 2F, and S2C), and wild-type RRM2

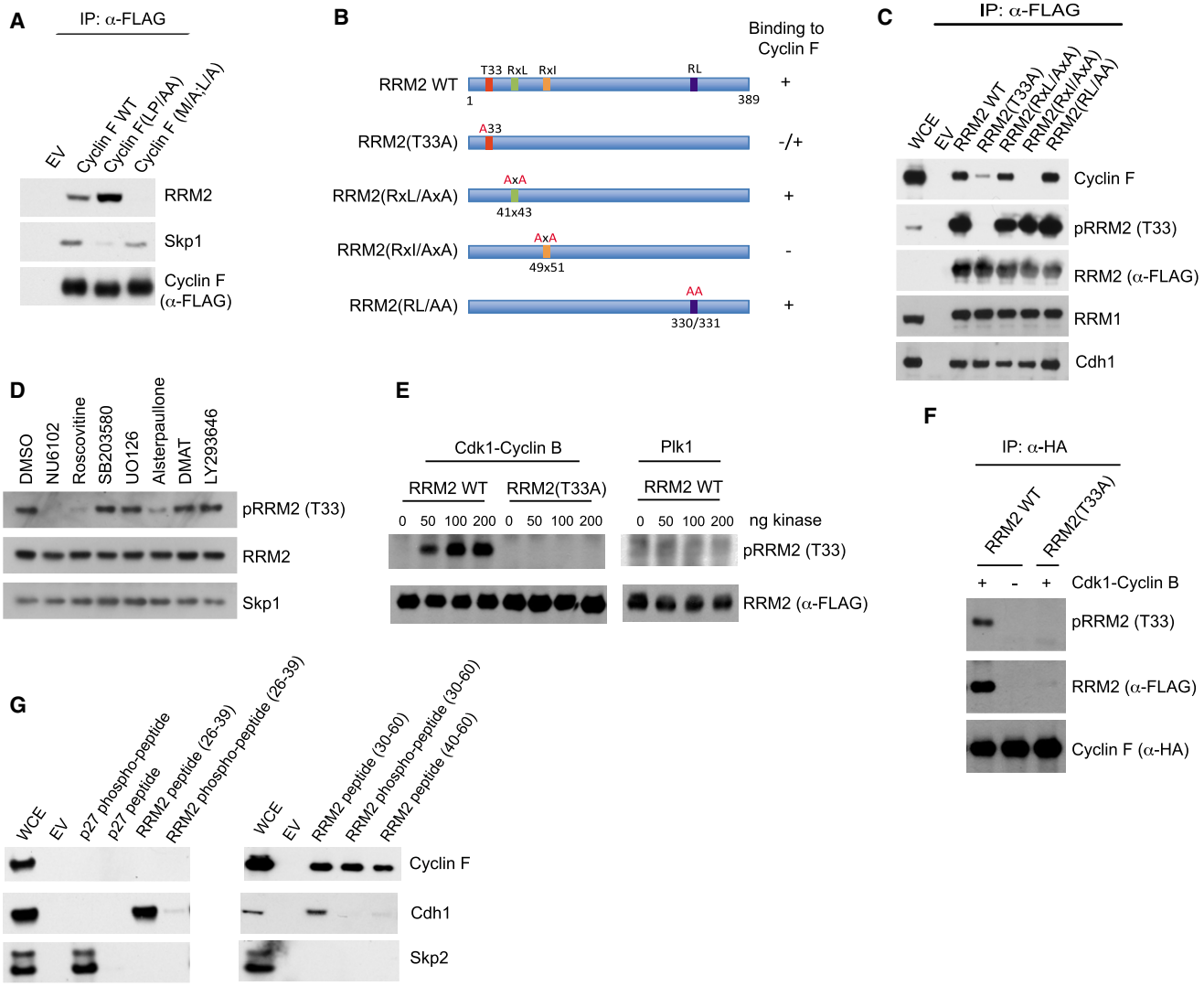

Figure 2. Both a CY Motif and the Phosphorylation of Thr33 in RRM2 Are Required for RRM2 Binding to cyclin F

(A) HEK-293T cells were transfected with either an empty vector (EV), FLAG-tagged cyclin F, or the indicated FLAG-tagged cyclin F mutants. Whole-cell extracts were immunoprecipitated (IP) with anti-FLAG resin, and immunocomplexes were immunoblotted as indicated.

(B) Schematic representation of RRM2 mutants highlighting putative cyclin F binding motifs in RRM2. RRM2 mutants that interacted with endogenous cyclin F are designated with the symbol (+).

(C) HEK-293T cells were transfected with either an empty vector (EV), FLAG-tagged RRM2, or the indicated FLAG-tagged RRM2 mutants. Whole-cell extracts were immunoprecipitated (IP) with anti-FLAG resin, and immunocomplexes were immunoblotted as indicated.

(D) HeLa cells were treated with the indicated kinase inhibitors. Cells were collected 4 hr later, lysed, and immunoblotted as indicated.

(E) In vitro transcribed/translated RRM2 was incubated at 30°C with the indicated amounts of either Cdk1-cyclin B complex (upper panels) or Plk1 (bottom panels). After 30 min, reactions were stopped, and samples were immunoblotted as indicated.

(F) In vitro-transcribed/translated RRM2 or RRM2(T33A) were incubated at 30°C in the presence or absence of Cdk1-cyclin B. After 30 min, in vitro transcribed/translated HA-cyclin F was added to the reaction and incubated for an additional 30 min. Cyclin F was then immunoprecipitated with an anti-HA antibody, and immunocomplexes were immunoblotted as indicated.

(G) HeLa cell extracts were incubated with beads coupled to the following peptides: RRM2 (26–39) (SLVDKENTPPALSG), phospho-RRM2 (26–39) (SLVDKENTp-PPALSG), RRM2 (30–60) (KENTPPALSGTRVLASKTARRIFQEPTEPK), phospho-RRM2 (30–60) (KENTp-PPALSGTRVLASKTARRIFQEPTEPK), RRM2 (40–60) (TRVLASKTARRIFQEPTEPK), p27 (180–198) (NAGSVEQTPKKPGLRRRQT), or phospho-p27 (180–198) (NAGSVEQTp-PKKPGLRRRQT). Beads were extensively washed, and bound proteins were immunoblotted as indicated.

See also Figures S1 and S2.

was unable to bind cyclin F in vitro without prior phosphorylation by a CDK (Figure 2F). However, RRM2(RxI/AxA), in which Thr33 is intact, was unable to bind cyclin F, even though phosphorylation of Thr33 was unaffected (Figure 2C), and a peptide corresponding to amino acids 26–39 of RRM2 (i.e., a peptide that does not contain the CY motif) was unable to bind cyclin F irrespective

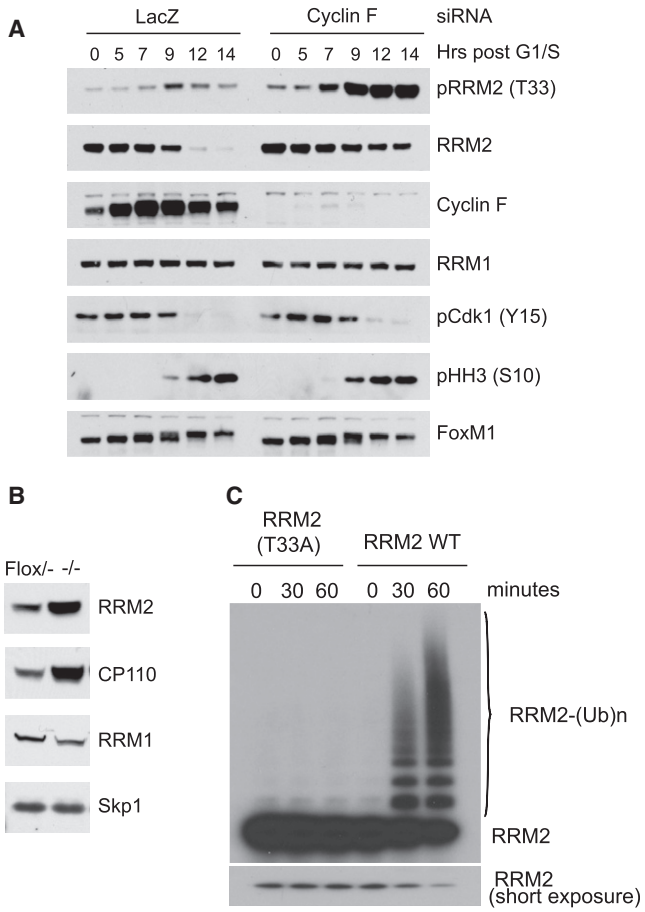

Figure 3. RRM2 Is Targeted for Ubiquitylation and Degradation by SCF$^{cyclin\ F}$

(A) HeLa cells were transfected with siRNAs to either a nonrelevant mRNA (LacZ) or cyclin F mRNA. Cells were synchronized at G1/S by a double-thymidine block and collected at the indicated time points after release from the block. Cell lysates were immunoblotted as indicated.

(B) *Cyclin F−/−* and parental *Cyclin F$^{Flox/-}$* MEFs were lysed and immunoblotted as indicated.

(C) ^{35}[S]-in vitro-translated RRM2 or RRM2(T33A) were incubated at 30°C with Cdk1-cyclin B and then, for the indicated times, with a ubiquitylation mix containing purified, recombinant SCF$^{cyclin\ F}$. Reactions were analyzed by autoradiography. The bracket indicates a ladder of bands corresponding to polyubiquitylated RRM2.

See also Figure S3.

of the Thr33 phosphorylation state (Figure 2G). Notably, whereas neither domain was sufficient for cyclin F binding, several lines of evidence indicate that phosphorylation of RRM2 on Thr33 does not provide an interface for cyclin F binding and instead exposes the CY motif at residues 49–51 for cyclin F recognition: (1) a peptide corresponding to amino acids 30–60 of RRM2 was able to bind cyclin F irrespective of the Thr33 phosphorylation state (Figure 2G); (2) a peptide corresponding to amino acids 40–60 of RRM2 was able to efficiently bind cyclin F (Figure 2G); and (3) RRM2(40–389), a mutant in which the first 39 amino acids were deleted, interacted with cyclin F in vivo as efficiently as wild-type RRM2 (Figure S2B). Thus, when the first 30–40 amino acids of cyclin F are deleted (and the CY motif at 49–51 is presumably exposed), Thr33 becomes dispensable.

RRM2 Is Targeted for Degradation by SCF$^{Cyclin\ F}$

We noted that, compared to wild-type cyclin F, the cyclin F(LP/AA) mutant (in which the first two amino acids of the F-box domain were mutated to alanine) bound less Skp1 and Cul1 (as expected) and more RRM2 (Figure 2A). This result suggested that RRM2 is targeted for proteolysis by cyclin F because this mutant is unable to form an active SCF ubiquitin ligase and can sequester RRM2. To test whether cyclin F regulates the degradation of RRM2, we used three established siRNA oligos (D'Angiolella et al., 2010) to reduce the expression of cyclin F in synchronized HeLa cells. We also silenced Cyclin F expression in synchronized U-2OS and RPE1-hTERT cells by using the most effective of the three oligos. In all cases, depletion of cyclin F inhibited the G2-specific degradation of RRM2 (Figures 3A and S3A and data not shown). Significantly, compared to controls, the amount of RRM2 phosphorylated on Thr33 drastically increased, confirming that it is the phosphorylated form of RRM2 that is targeted by SCF$^{cyclin\ F}$. Upon cyclin F depletion in G2 cells, RRM2 half-life increased (Figure S3B) and RRM2 accumulated mostly in the cytoplasm because of active nucleus-cytoplasm shuttling, as indicated by its nuclear accumulation following LMB treatment (Figure S3C). Moreover, in agreement with the siRNA results, we observed that *Cyclin F−/− m*ouse *e*mbryonic *f*ibroblasts (MEFs) (Tetzlaff et al., 2004) displayed RRM2 accumulation compared to parental *Cyclin F$^{Flox/-}$* MEFs (Figure 3B). Finally, purified wild-type cyclin F, but not cyclin F(LP/AA), promoted the in vitro ubiquitylation of RRM2, but not RRM2(T33A) (Figures 3C and S3D and S3E), supporting the hypothesis that cyclin F directly controls the ubiquitin-mediated degradation of RRM2.

Cyclin F-Mediated Degradation of RRM2 Prevents Genome Instability

Together, the results shown in Figures 1, 2, 3, S1, S2, and S3 demonstrate that cyclin F mediates the nuclear degradation of RRM2 in G2. To investigate the biological significance of this event, we analyzed synchronized HeLa, U-2OS, and RPE1-hTert cells expressing either HA-tagged wild-type RRM2, HA-tagged RRM2(RxI/AxA), or HA-tagged RRM2(T33A). In G2 and M, wild-type RRM2 was degraded, whereas RRM2(RxI/AxA) and RRM2(T33A) were not (Figures 4A and 4BB and S4A–S4C), in agreement with their inability to efficiently bind cyclin F (Figure 2C). Importantly, the expression of stable RRM2 mutants induced an increase in the cellular concentration of dATP and dGTP, but not dCTP and dTTP (Figures 4C and S4D), creating an imbalance in dNTP pools. This result is consistent with a reduction of purine dNTPs, but not pyrimidine dNTPs, in cells treated with either hydroxyurea, an RNR inhibitor, or an siRNA to RRM2 (Håkansson et al., 2006; Lin et al., 2007; Lin et al., 2004), and it is likely due to a more efficient nucleotide salvage pathway for pyrimidine deoxyribonucleosides than purine deoxyribonucleosides (Reichard, 1988).

We also synchronized in prometapahse RPE1-hTert cells infected with either an empty retrovirus or a retrovirus expressing HA-tagged wild-type RRM2, HA-tagged RRM2(T33A), or

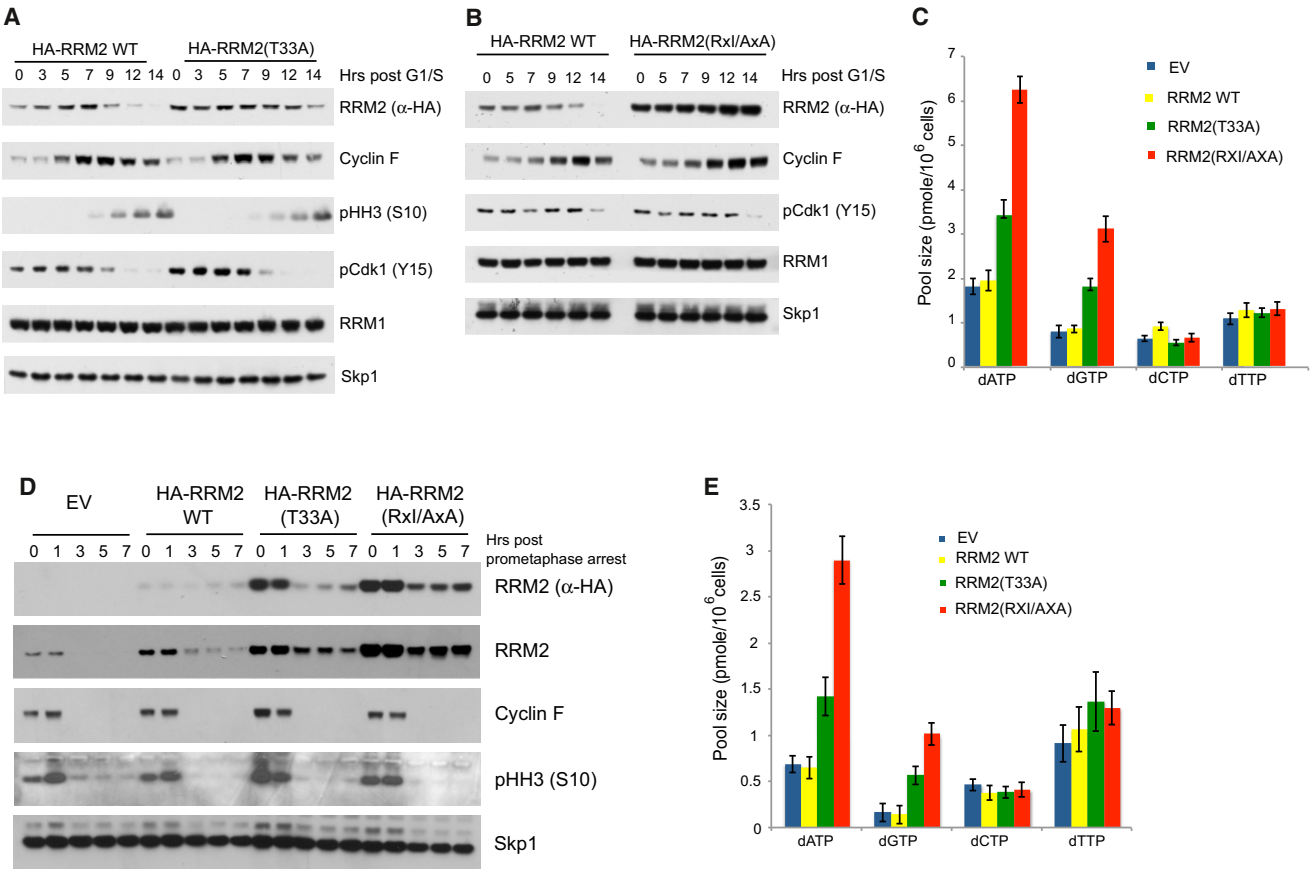

Figure 4. Expression of Stable RRM2 Mutants Induces an Increase in the Concentration of dATP and dGTP

(A) HeLa cells infected with either a retrovirus expressing HA-tagged RRM2 or HA-tagged RRM2(T33A) were synchronized by using a double-thymidine block. Samples were collected at the indicated times after release, lysed, and immunoblotted as indicated.

(B) HeLa cells infected with either a retrovirus expressing HA-tagged RRM2 or HA-tagged RRM2(RxI/AxA) were analyzed as in (A).

(C) RPE1-hTert cells infected with either a retrovirus expressing HA-tagged RRM2, HA-tagged RRM2(T33A), or HA-tagged RRM2(RxI/AxA) were enriched for the G2 and M populations and lysed to assess the concentration of dNTPs. Each data point represents the mean ± standard deviation (SD) of three separate experiments.

(D) RPE1-hTert cells infected with either an empty virus (EV) or a retrovirus expressing HA-tagged wild-type (WT) RRM2, HA-tagged RRM2(T33A), or HA-tagged RRM2(RxI/AxA) were incubated for 16 hr with nocodazole and subjected to a mitotic shake-off to isolate round, prometaphase cells, which were subsequently released into fresh medium. Samples were collected at the indicated times after release from the block, lysed, and immunoblotted as indicated.

(E) RPE1-hTert cells were treated as in (D). Three hours after release from the prometaphase arrest, cells were lysed to quantify dNTP concentrations. Each data point represents the mean ± SD of three separate experiments.

See also Figure S4.

HA-tagged RRM2(RxI/AxA) (Figure 4D). Cells were released from the block, and, 3 hr after, the majority of cells were in G1, as indicated by the disappearance of Histone H3 phosphorylated on Ser10. In all cases, when cells reached the next G1, the levels of both endogenous and exogenous RRM2 decreased (Figure 4D), likely due to APC/C^{Cdh1} (Chabes et al., 2003b), which does not require either T33 or the RxI motif to interact with RRM2 (Figures 2C and 2G). Yet, in G1, levels of RRM2(T33A) and RRM2(RxI/AxA) remained higher than endogenous RRM2 (Figure 4D). Consistent with this observation, the concentrations of purine dNTPs were higher in G1 cells expressing stable RRM2 mutants compared to wild-type cells (Figure 4E).

Failures in the control of dNTP levels have been shown to lead to genome instability (Chabes et al., 2003a; Hu and Chang, 2007; Ke et al., 2005; Kunz, 1988; Kunz et al., 1994; Meuth, 1989; Phear and Meuth, 1989; Xu et al., 2008). To test whether expression of the RRM2 mutants induced mutations, we measured the spontaneous mutation frequency of the gene encoding hypoxanthine phosphoribosyl transferase (*HPRT*). Because of the presence of HPRT, cells are sensitive to 6-thioguanine (6-TG), thus, the occurrence of resistant clones represents spontaneous mutations at the *HPRT* locus (Darè et al., 1995). Upon 6-TG selection, and after adjusting for plating efficiency, we observed that, compared to cells transfected with an empty vector or expressing wild-type RRM2, cells expressing stable RRM2 mutants developed approximately 20 and 40 times more resistant colonies, respectively (Figure 5A), corresponding to 20- and 40-fold increases in mutation frequency.

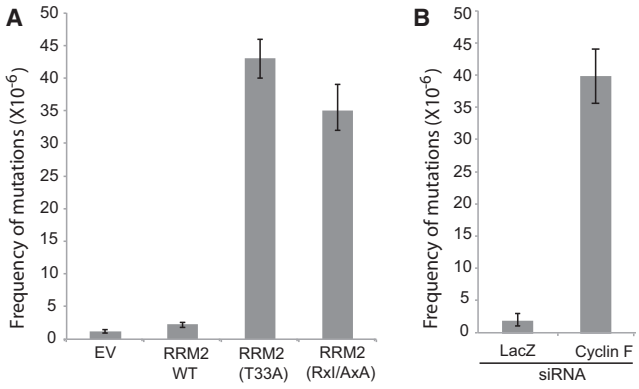

Figure 5. Cyclin F-Mediated Degradation of RRM2 Prevents Genome Instability

(A) The frequency of mutations at the *HPRT* locus was determined in U-2OS cells infected with a retrovirus expressing either RRM2 or the indicated HA-tagged RRM2 mutants. Each data point represents the mean ± SD of three separate experiments.

(B) The frequency of mutations at the *HPRT* locus was determined in U-2OS cells transfected with siRNAs to either a nonrelevant mRNA (LacZ) or cyclin F mRNA. Each data point represents the mean ± SD of three separate experiments.

These experiments show that the regulation of RRM2 degradation via cyclin F is required to maintain dNTP pool balance and prevent genome instability. Accordingly, cyclin F silencing mimicked the phenotypes observed following expression of stable RRM2 mutants (i.e., unbalanced dNTP pools and increased rate of mutation) (Figures 5B and S4E).

Finally, we generated and sequenced *HPRT* cDNAs from 21 individual 6-TG resistant clones expressing stable RRM2 mutants. Mutations, including deletions, transversions, transitions, and insertions were found in all 21 HPRT coding sequences in these clones. Interestingly, 15 of the 21 clones analyzed showed skipping of exon 8. This deletion has been reported to depend on mutations in the pyrimidine rich tract of intron 7 (Andersson et al., 1992), which is consistent with the increased levels of purines detected in cells expressing stable RRM2 or depleted of cyclin F (Figures 4C, 4E, and S4D).

Upon Genotoxic Stress, Cyclin F Is Downregulated and RRM2 Accumulates in a ATR-Dependent Manner

In response to DNA damage, RRM2 is recruited to the nucleus to guarantee local availability of dNTPs for efficient DNA repair synthesis (Chabes and Thelander, 2000; Lin et al., 2007; Niida et al., 2010; Zhang et al., 2009). We found that, in any cell line tested, and in response to a number of DNA damaging agents (e.g., doxorubicin, CPT, UV-C, MMS, NCZ, or γ-irradiation), the levels of cyclin F drop, with coincident accumulation of RRM2 (Figures 6A and 6B, and data not shown). These changes were not due to changes in cell-cycle distribution (Figure S5A) and, in fact, similar protein oscillations were observed in cells synchronized in G2 (Figures S5B and S5C). These events appeared to be dependent on ATM and/or ATR, as caffeine inhibited both cyclin F degradation and RRM2 accumulation (Figure 6A). We then observed that cyclin F was still degraded and RRM2 was still upregulated in immortalized fibroblasts obtained from Ataxia Telangiectasia (AT) patients (Figure 6C), which carry a mutated ATM gene. In contrast, when ATR was ablated from HCT116 ATR$^{Flox/-}$ cells (Cortez et al., 2001; Martin et al., 2011); this response was deficient (Figure 6D). Finally, we excluded that this function is mediated by CHK1, a kinase activated by ATR because silencing CHK1 expression did not affect cyclin F downregulation (Figure S5D). Thus, cyclin F downregulation is mediated by ATR, but not ATM, in a Chk1-independent manner.

The downregulation of cyclin F protein in response to genotoxic stress was at least partially due to degradation. In fact, whereas the levels and stability of cyclin F mRNA did not change significantly after DNA damage, treatment of cells with the proteasome inhibitor MG132 prevented the disappearance of cyclin F (Figures S6A and S6B). When expressed at near physiologic levels, exogenous cyclin F was downregulated similar to the endogenous protein (Figure S6C). Analysis of the stability of different truncation mutants suggested that cyclin F downregulation upon DNA damage depends on a motif located between amino acids 407 and 660 (data not shown) and a cyclin F fragment encompassing amino acids 407–660 was able to transfer DNA damage-dependent instability to GFP (Figure S6D). This domain contains three SerGln (526, 534, 595) and four ThrGln sites (427, 467, 472, 543), which are potential sites of phosphorylation by ATR, and although two of these seven sites are conserved in mammals, none are conserved throughout vertebrates. Mutation of these seven residues to Ala did not abrogate the sensitivity of cyclin F to genotoxic stress (Figure S6C), suggesting the effect of ATR on cyclin F stability is indirect.

Cyclin F Downregulation Is Required for Efficient DNA Repair

In agreement with previous reports (Niida et al., 2010; Xu et al., 2008; Xue et al., 2003; Zhang et al., 2009), we found that in response to genotoxic stress, RRM2 accumulates in the nucleus, as detected by immunofluorescence staining of U-2OS cells (Figure S7A) or immunoblotting of the chromatin fractions from either HeLa or RPE1-hTERT cells (Figures 7A and S7B). Thus, we hypothesized that cyclin F downregulation is a prerequisite for the accumulation of nuclear RRM2. To test this hypothesis, we either infected HeLa cells with doxycycline-repressible cyclin F constructs [wild-type cyclin F, cyclin F(M309A)])(Figure 7A) or transiently expressed wild-type cyclin F in RPE1-hTERT cells (Figure S7B), and subjected them to various forms of DNA damage. In contrast to control cells, RRM2 failed to accumulate in cells expressing wild-type cyclin F, whereas cells expressing the inactive cyclin F(M309A) mutant retained the ability to accumulate nuclear RRM2.

We then performed alkaline comet assays to monitor DNA repair and found that cells expressing wild-type cyclin F, but not cyclin F(M309A), displayed a reduced ability to repair damaged DNA (Figure 7B). Accordingly, compared to control cells, many more cells died (as judged by clonogenic survival) after UV treatment when expression of wild-type cyclin F, but not cyclin F(M309A) or cyclin F(LP/AA), was induced in HeLa cells by removing doxycycline (Figures 7C and S7C). Significantly, expression of a stable RRM2 mutant [either

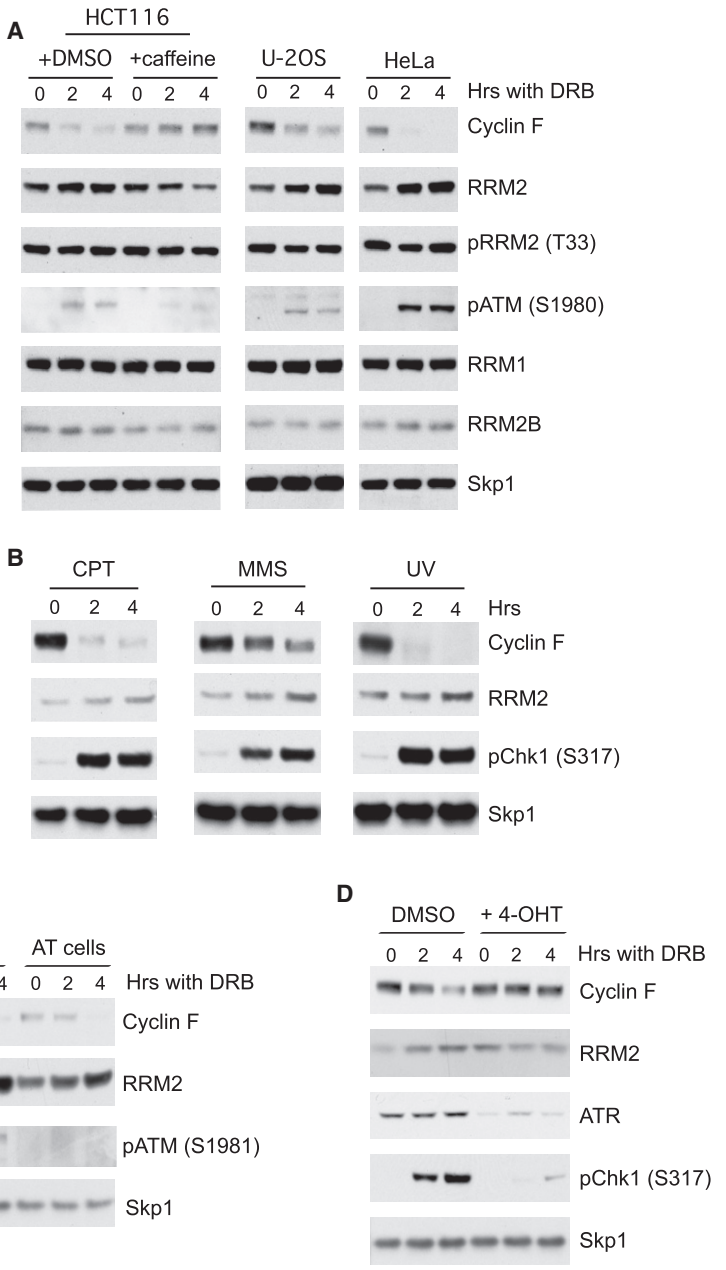

Figure 6. Upon Genotoxic Stress, Cyclin F Is Downregulated and RRM2 Accumulates in a ATR-Dependent Manner

(A) HCT116, U-2OS, and HeLa cells were treated with doxorubicin (DRB) for the indicated times. After DRB treatment, cells were collected, lysed, and immunoblotted as indicated.

(B) HeLa cells were treated with the indicated DNA damaging agents: or (camptothecin), MMS (methyl methanesulfonate), UV (8 J/m^2). Cells were collected at the indicated times after treatment, lysed, and immunoblotted as indicated.

(C) Normal Human Fibroblasts immortalized with hTert (NHFs) and GM0252A-hTert fibroblasts from an ataxia-teleangectasia patient (AT cells) were treated with DRB. Cells were collected at the indicated times after treatment, lysed, and immunoblotted as indicated.

(D) HCT116 *ATR* Flox/− cells were incubated with 4-OHT (4-hydroxytamoxifen) for 24 hr (to induce ATR ablation) and then with doxorubicin (DRB). Cells were collected at the indicated times after DRB treatment, lysed, and immunoblotted as indicated.

See also Figures S5 and S6.

RRM2(RxI/AxA) or RRM2(T33A)], but not wild-type RRM2, reverted the UV sensitivity induced by the expression of cyclin F (Figure 7D and data not shown), indicating that the downregulation of cyclin F after genotoxic stress is required to allow RRM2 accumulation within the nucleus and, consequently, efficient DNA repair.

DISCUSSION

Here we report that RRM2 is targeted for degradation by SCF$^{\text{cyclin F}}$ during the G2 phase of the cell cycle (see model in Figure 7E). Failure to degrade RRM2 in G2 promotes imbalances in dNTP pools (both at G2/M and during the next G1) and an increased frequency of mutations (Figures 4, 5, and S4). Imbalances in dNTP pools result in increased base misincorporation during DNA synthesis and decreased proofreading due to enhanced polymerization rates (Mathews, 2006). Abnormal dNTP levels negatively affect the fidelity of DNA replication, producing an increase in gene mutation rate and genome instability. In agreement with these data, (1) elevated or imbalanced pools of dNTPs promote transformation and induce an increase in the rate of spontaneous mutations in cell systems (Chabes et al., 2003a; Hu and Chang, 2007; Ke et al., 2005; Kunz, 1988; Kunz et al., 1994; Meuth, 1989; Phear and Meuth, 1989), (2) overexpression of RRM2 induces the development of lung cancer in mice (Xu et al., 2008), and (3) elevated levels of RRM2 correlate with poor prognoses for cancer patients (Ferrandina et al., 2010; Grade et al., 2011; Jones et al., 2011; Kretschmer et al., 2011; Morikawa et al., 2010a; Morikawa et al., 2010b; Satow et al., 2010).

Oncogenic stress produces dNTP deficiencies and a consequent DNA replication stress typical of early oncogenic events (Bester et al., 2011). In contrast, expression of an RRM2 stable mutant increases the dNTP pool, but it does not induce DNA replication stress, as indicated by the lack of Chk1 phosphorylation or induction of 53BP1 bodies in G1 nuclei (Figure S4A and data not shown) (G1 nuclear 53BP1 bodies mark DNA lesions induced by replication stress [Lukas et al., 2011]). These findings suggest that mammalian cells may not have a checkpoint that senses dNTP pool increases, highlighting the risk of elevated RRM2 levels for the pathogenesis of cancer.

An interesting aspect of RRM2 degradation via SCF$^{\text{cyclin F}}$ is its regulation by CDKs. In fact, although cyclin F utilizes its

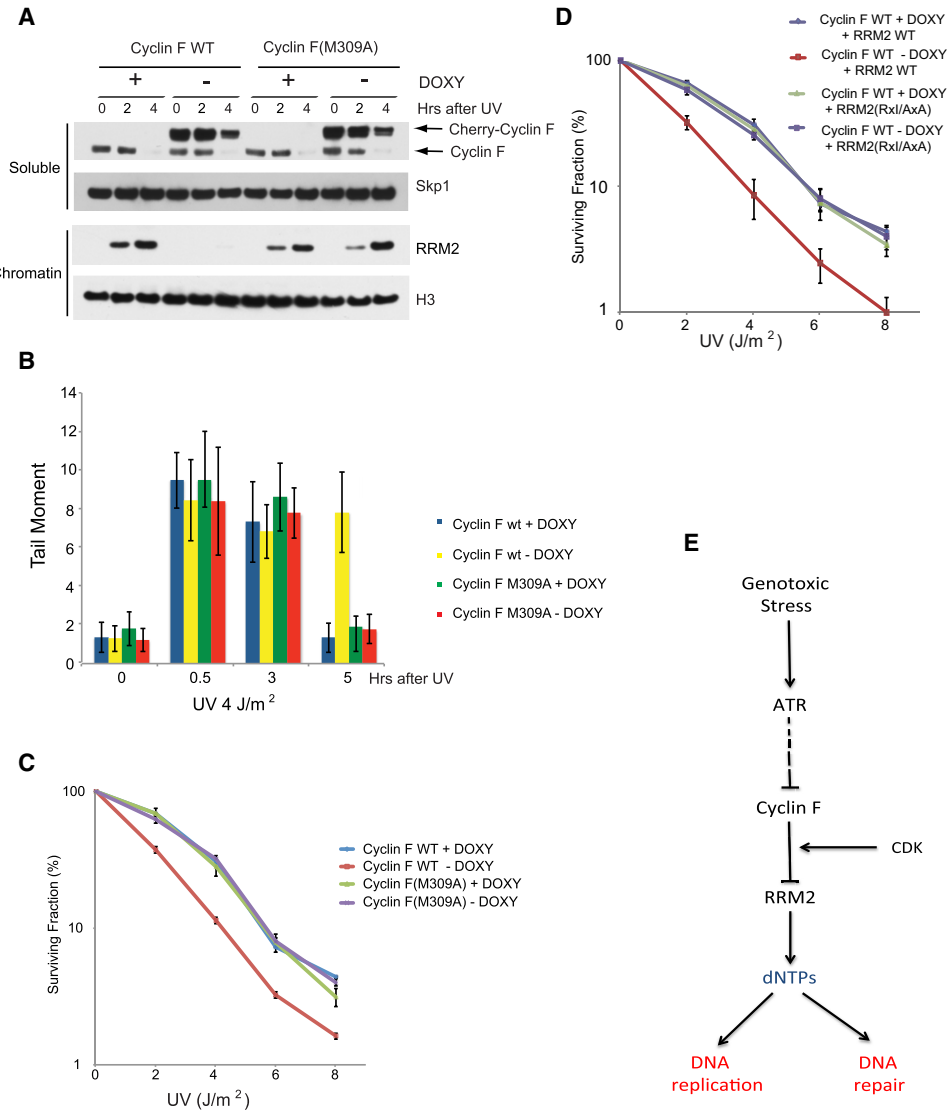

Figure 7. Cyclin F Downregulation Is Required for Efficient DNA Repair

(A) HeLa cells infected with a pLVX Tet-Off lentivirus and either pLVX-Tight-puro Cherry-cyclin F or pLVX-Tight-puro Cherry-cyclin F(M309A) lentiviruses were treated with or without doxycyclin (DOXY) for 48 hr. Next, cells were treated with UV (4 J/m^2) for the indicated times. After treatment, cell pellets were divided into chromatin and soluble fractions and immunoblotted as indicated.

(B) HeLa cells treated as in (A) were subjected to alkaline comet assays. Each data point represents the mean ± SD of three separate experiments in which at least 100 cells per sample were counted.

(C) HeLa cells were treated as in (A), except that the indicated doses of UV were used. A colony formation assay was performed 10 days after treatment. Each data point represents the mean ± SD of three separate experiments.

(D) HeLa cells preinfected with either pBabe HA-tagged RRM2 or pBabe HA-tagged RRM2(RxI/AxA) were infected as described in (A), and exposed to the indicated UV doses. A colony formation assay was performed 10 days after treatment. Each data point represents the mean ± SD of three separate experiments.

(E) A model of the regulation of DNA replication and repair by the cyclin F-RRM2 axis. During G2, after the last majority of DNA replication has occurred, cyclin F accumulates, thereby promoting RRM2 degradation in collaboration with a G2 CDK. DNA damage induces a ATR-dependent downregulation of cyclin F to allow accumulation of RRM2 for efficient DNA repair.

See also Figure S7.

hydrophobic patch to recognize the CY motif in RRM2 (similar to other cyclin-substrate pairs), it does so only after RRM2 is phosphorylated by CDKs on Thr33, an event that appears to expose the CY motif (Figure 2 and S2B). Thus, the mode of RRM2 recognition by cyclin F is an exception to the rule that cyclin-substrate interactions do not require posttranslational modifications, highlighting the unique nature of RRM2 regulation. Interestingly, RRM2 is also phosphorylated by CDKs on Ser20 (Chan et al., 1993; Chan et al., 1999). However, in contrast to Thr33 phosphorylation, this modification occurs early in S phase, does not

affect RRM2 stability, and its function remains unknown (Chabes and Thelander, 2000).

After genotoxic stress, the levels of cyclin F in both p53-positive and p53-negative cells rapidly drop, allowing the recruitment of RRM2 to chromatin for efficient DNA repair synthesis (Figures 6, 7E, S5, and S6). This function is consistent with reports indicating a role for RNR in guaranteeing availability of dNTPs at the sites of DNA damage (Lin et al., 2007; Niida et al., 2010; Zhang et al., 2009). The timing of RRM2 accumulation following DNA damage parallels the timing of DNA repair (Figures 6, 7A, and 7B). The rapid accumulation of RRM2 protein requires cyclin F downregulation, which occurs in an ATR-dependent, but Chk1- and transcription-independent, manner (Figures 6 and S5C and S5D). However, if DNA damage persists, RRM2 upregulation also relies on Chk1- and E2F1-dependent transcription (Zhang et al., 2009). Moreover, upon persistent genotoxic stress, a different RNR subunit, called RRM2B or p53R2 (which normally substitutes for RRM2 to form an active RNR complex necessary for the synthesis of mitochondrial DNA [Bourdon et al., 2007; Wang et al., 2011]), accumulates much later (48–72 hr later) after DNA damage in a p53-dependent manner (Håkansson et al., 2006; Tanaka et al., 2000).

We have previously shown that cyclin F controls centrosome duplication and prevents chromosome instability by promoting the degradation of CP110 (D'Angiolella et al., 2010). Our current study reveals that cyclin F controls the cellular dNTP pools and prevents genome instability by promoting RRM2 degradation. Thus, cyclin F is a hub that coordinates and synchronizes centrosome duplication with DNA replication to ensure proper cell division. Interestingly, hydroxyurea (HU) inhibits RNR and induces centrosome duplication in certain cell types (Balczon et al., 1995; Meraldi et al., 1999). The fact that cyclin F, but not CP110, is degraded after HU treatment (D'Angiolella et al., 2010) may explain why HU (by blocking RNR) induces dissociation of centrosome duplication from DNA replication.

In addition to the fundamental implications for our understanding of cell physiology, our studies have clinical relevance because they provide insight into the response to genotoxic stress caused by HU, gemcitabine, fludarabine phosphate, and cladribine, RNR-inhibiting drugs that are used in the treatment of various cancers, including leukemia, melanoma, metastatic ovarian cancer, nonsmall cell lung cancer, and pancreatic cancer (Shao et al., 2006). Moreover, because the failure to downregulate cyclin F in response to DNA damage blocks nuclear accumulation of RRM2 and induces cell death, we propose that the inhibition of cyclin F degradation may be useful for enhancing the chemosensitivity of cancer cells to DNA damage-based therapies.

EXPERIMENTAL PROCEDURES

Biochemical Methods

Extract preparation, immunoprecipitation, and immunoblotting have been previously described (Bassermann et al., 2008; Guardavaccaro et al., 2008). Subcellular fractionation was performed as described (Ballabeni et al., 2004). Briefly, Soluble fraction was extracted by using CSK buffer (0.5% Triton X-100, 10 mM Pipes [pH 6.8], 100 mM NaCl, 1.5 mM $MgCl_2$, 300 mM sucrose, 1 mM aprotinin, 1 mM leupeptin, and 1 mM PMSF). Cells lysates were centrifuged at 1,700 rcf for 4 min. After centrifugation, cell pellets were washed and insoluble proteins were extracted by using CSK buffer containing 250 mM NaCl and Turbo Nuclease (Accelagen).

Purification and MudPIT Analysis

HEK293T cells were transfected with constructs encoding either FLAG-HA-tagged cyclin F or FLAG-HA-tagged cyclin F(1-270). Cell lysis, immunopurification, and MS/MS analysis have been previously described (D'Angiolella et al., 2010).

Immunofluorescence Microscopy

Cells were fixed with PFA 4% for 10 min, permeabilized with PBS containing 1% Triton X-100 for 10 min and blocked for 1 hr in PBS containing 0.1% Triton X-100 3% BSA prior to incubation with primary antibodies. (Please note that PFA does not allow detection of centrosomal cyclin F.) Secondary antibodies were from donkey and conjugated with Alexa Fluor fluorochromes (Invitrogen). DAPI was used to stain DNA. Slides were mounted with Prolong-Gold (Invitrogen). Confocal microscopy was performed by using a Zeiss LSM 510, equipped with Zeiss LSM 510 software.

Establishment of Tet-Off HeLa Cells Expressing Cherry Cyclin F and pBABE HA-Tagged RRM2

pLVX-Tight-puro Cherry-cyclin F, pLVX-Tight-puro Cherry-cyclin(FM309A), pLVX Tet-Off lentiviruses were produced according to the manufacturer instruction (Clontech). HeLa cells (preinfected or not with pBABE vectors expressing wild-type or mutant RRM2) were infected with lentiviruses; positive clones were selected by using puromycin (1 μg/ml) and G418 (800 μg/ml), and grown in the presence of Doxycycline (2 μg/ml). Doxycycline removal induced Cherry-cyclin F expression.

Gene Silencing by Small Interfering RNA

The sequences of the oligonucleotides numbers 1, 2, and 3, corresponding to the cyclin F mRNA, were CCAGUUGUGUGCUGCAUUA, UAGCCUACCU CUACAAUGA, and GCACCCGGUUUAUCAGUAA, respectively. A dsRNA oligo to LacZ mRNA (CGUACGCGGAAUACUUCGA) served as a negative control (Duan et al., 2012).

Determination of dNTP Pool in Whole-Cell Extracts

U-2OS and RPE1-hTERT cells (5×10^6) were washed twice with cold PBS and extracted by using 1 ml of ice-cold 60% methanol for 1 hr at −20°C, followed by centrifugation for 15 min at 14,000 × g. The supernatant was dried under vacuum; the pellet was dissolved in 200 μl of sterile water and stored at −20°C. Determination of the dNTP pool size was based on DNA polymerase-catalyzed incorporation of radioactive dNTP into the synthetic oligonucleotide template as described (Sherman and Fyfe, 1989).

Determination of Mutation Rates

For stable transfection U-2OS cells were infected with pBABE retroviruses expressing HA-tagged RRM2, HA-tagged RRM2(T33A), and HA-tagged RRM2(RxI/AxA). After infection, cells were selected by using puromycin for 2 days. Mutation frequencies were determined by *HPRT* mutation as described (Xu et al., 2008). 6-TG resistant clones were subcultured in 24-well format. When individual clones reached confluence, RNA was extracted and cDNA was synthesized with Fast Lane cDNA synthesis kit (QIAGEN), according to manufacturer's instruction. The *HPRT* open reading frame was PCR amplified by using the following primers: 5′-CTGAGCAGT CAGCCCGCG-3′ and 5′-GAGAATTTTTTCATTTACAAGTTAAACAACAATCC GCC-3′. *HPRT* mutations were identified vis direct sequencing of PCR products by using the following primers: 5′-CGCCGGCCGGCT-3′ and 5′-GGCTCATAGTGCAAATAAACA-3′.

Comet Assay

Alkaline comet assays were performed by using a Trevigen's Comet Assay kit (4250-050-k) according to the manufacturer's instructions. DNA was stained with SYBR Green, and slides were photographed by using a Zeiss Axiovert 200 M microscope, equipped with a cooled Retiga 2000R CCD (QImaging). Tail moments were analyzed as reported previously (Park et al., 2006) by using the Tritek Comet Score Freeware.

Clonogenic Assay

Tet-off HeLa cells expressing Cherry-cyclin F or Cherry-cyclin F(M309A) were irradiated with varying doses of UV-C in the presence or absence of doxycycline (2 μg/ml) and then washed with PBS. Ten days after an additional incubation, surviving colonies were counted and their relative numbers were expressed as percentages of the untreated cells as described (Franken et al., 2006).

SUPPLEMENTAL INFORMATION

Supplemental Information includes Extended Experimental Procedures, seven figures, and one table and can be found with this article online at doi:10.1016/j.cell.2012.03.043.

ACKNOWLEDGMENTS

The authors thank S. Elledge, L. Gardner and N. Zheng for reagents, V. Bianchi for suggestions, and J.R. Skaar for reading the manuscript. M.P. is grateful to T.M. Thor for continuous support. V.D'A. was a Leukemia and Lymphoma Society Scholar. V.D'A. and V.D. received support from the American Italian Cancer Foundation. This work was supported by grants from the National Institutes of Health to M.P. (R01-GM057587, R37-CA076584, and R21-CA161108). A.S., L.F., and M.P.W. are supported by the Stowers Institute for Medical Research. M.P. is an Investigator with the Howard Hughes Medical Institute.

Received: November 17, 2011
Revised: February 1, 2012
Accepted: March 24, 2012
Published: May 24, 2012

REFERENCES

Andersson, B., Hou, S.M., and Lambert, B. (1992). Mutations causing defective splicing in the human hprt gene. Environ. Mol. Mutagen. *20*, 89–95.

Bai, C., Sen, P., Hofmann, K., Ma, L., Goebl, M., Harper, J.W., and Elledge, S.J. (1996). SKP1 connects cell cycle regulators to the ubiquitin proteolysis machinery through a novel motif, the F-box. Cell *86*, 263–274.

Balczon, R., Bao, L., Zimmer, W.E., Brown, K., Zinkowski, R.P., and Brinkley, B.R. (1995). Dissociation of centrosome replication events from cycles of DNA synthesis and mitotic division in hydroxyurea-arrested Chinese hamster ovary cells. J. Cell Biol. *130*, 105–115.

Ballabeni, A., Melixetian, M., Zamponi, R., Masiero, L., Marinoni, F., and Helin, K. (2004). Human geminin promotes pre-RC formation and DNA replication by stabilizing CDT1 in mitosis. EMBO J. *23*, 3122–3132.

Bassermann, F., Frescas, D., Guardavaccaro, D., Busino, L., Peschiaroli, A., and Pagano, M. (2008). The Cdc14B-Cdh1-Plk1 axis controls the G2 DNA-damage-response checkpoint. Cell *134*, 256–267.

Bester, A.C., Roniger, M., Oren, Y.S., Im, M.M., Sarni, D., Chaoat, M., Bensimon, A., Zamir, G., Shewach, D.S., and Kerem, B. (2011). Nucleotide deficiency promotes genomic instability in early stages of cancer development. Cell *145*, 435–446.

Bourdon, A., Minai, L., Serre, V., Jais, J.P., Sarzi, E., Aubert, S., Chrétien, D., de Lonlay, P., Paquis-Flucklinger, V., Arakawa, H., et al. (2007). Mutation of RRM2B, encoding p53-controlled ribonucleotide reductase (p53R2), causes severe mitochondrial DNA depletion. Nat. Genet. *39*, 776–780.

Cardozo, T., and Pagano, M. (2004). The SCF ubiquitin ligase: insights into a molecular machine. Nat. Rev. Mol. Cell Biol. *5*, 739–751.

Chabes, A., and Thelander, L. (2000). Controlled protein degradation regulates ribonucleotide reductase activity in proliferating mammalian cells during the normal cell cycle and in response to DNA damage and replication blocks. J. Biol. Chem. *275*, 17747–17753.

Chabes, A., Georgieva, B., Domkin, V., Zhao, X., Rothstein, R., and Thelander, L. (2003a). Survival of DNA damage in yeast directly depends on increased dNTP levels allowed by relaxed feedback inhibition of ribonucleotide reductase. Cell *112*, 391–401.

Chabes, A.L., Pfleger, C.M., Kirschner, M.W., and Thelander, L. (2003b). Mouse ribonucleotide reductase R2 protein: a new target for anaphase-promoting complex-Cdh1-mediated proteolysis. Proc. Natl. Acad. Sci. USA *100*, 3925–3929.

Chabes, A.L., Björklund, S., and Thelander, L. (2004). S Phase-specific transcription of the mouse ribonucleotide reductase R2 gene requires both a proximal repressive E2F-binding site and an upstream promoter activating region. J. Biol. Chem. *279*, 10796–10807.

Chan, A.K., Litchfield, D.W., and Wright, J.A. (1993). Phosphorylation of ribonucleotide reductase R2 protein: in vivo and in vitro evidence of a role for p34cdc2 and CDK2 protein kinases. Biochemistry *32*, 12835–12840.

Chan, A.K., Persad, S., Litchfield, D.W., and Wright, J.A. (1999). Ribonucleotide reductase R2 protein is phosphorylated at serine-20 by P34cdc2 kinase. Biochim. Biophys. Acta *1448*, 363–371.

Cortez, D., Guntuku, S., Qin, J., and Elledge, S.J. (2001). ATR and ATRIP: partners in checkpoint signaling. Science *294*, 1713–1716.

D'Angiolella, V., Donato, V., Vijayakumar, S., Saraf, A., Florens, L., Washburn, M.P., Dynlacht, B., and Pagano, M. (2010). SCF(Cyclin F) controls centrosome homeostasis and mitotic fidelity through CP110 degradation. Nature *466*, 138–142.

Darè, E., Zhang, L.H., Jenssen, D., and Bianchi, V. (1995). Molecular analysis of mutations in the hprt gene of V79 hamster fibroblasts: effects of imbalances in the dCTP, dGTP and dTTP pools. J. Mol. Biol. *252*, 514–521.

Daub, H., Olsen, J.V., Bairlein, M., Gnad, F., Oppermann, F.S., Körner, R., Greff, Z., Kéri, G., Stemmann, O., and Mann, M. (2008). Kinase-selective enrichment enables quantitative phosphoproteomics of the kinome across the cell cycle. Mol. Cell *31*, 438–448.

DeGregori, J., Kowalik, T., and Nevins, J.R. (1995). Cellular targets for activation by the E2F1 transcription factor include DNA synthesis- and G1/S-regulatory genes. Mol. Cell. Biol. *15*, 4215–4224.

Duan, S., Cermak, L., Pagan, J.K., Rossi, M., Martinengo, C., di Celle, P.F., Chapuy, B., Shipp, M., Chiarle, R., and Pagano, M. (2012). FBXO11 targets BCL6 for degradation and is inactivated in diffuse large B-cell lymphomas. Nature *481*, 90–93.

Emanuele, M.J., Elia, A.E., Xu, Q., Thoma, C.R., Izhar, L., Leng, Y., Guo, A., Chen, Y.N., Rush, J., Hsu, P.W., et al. (2011). Global identification of modular cullin-RING ligase substrates. Cell *147*, 459–474.

Ferrandina, G., Mey, V., Nannizzi, S., Ricciardi, S., Petrillo, M., Ferlini, C., Danesi, R., Scambia, G., and Del Tacca, M. (2010). Expression of nucleoside transporters, deoxycitidine kinase, ribonucleotide reductase regulatory subunits, and gemcitabine catabolic enzymes in primary ovarian cancer. Cancer Chemother. Pharmacol. *65*, 679–686.

Florens, L., and Washburn, M.P. (2006). Proteomic analysis by multidimensional protein identification technology. Methods Mol. Biol. *328*, 159–175.

Franken, N.A., Rodermond, H.M., Stap, J., Haveman, J., and van Bree, C. (2006). Clonogenic assay of cells in vitro. Nat. Protoc. *1*, 2315–2319.

Fung, T.K., Siu, W.Y., Yam, C.H., Lau, A., and Poon, R.Y. (2002). Cyclin F is degraded during G2-M by mechanisms fundamentally different from other cyclins. J. Biol. Chem. *277*, 35140–35149.

Grade, M., Hummon, A.B., Camps, J., Emons, G., Spitzner, M., Gaedcke, J., Hoermann, P., Ebner, R., Becker, H., Difilippantonio, M.J., et al. (2011). A genomic strategy for the functional validation of colorectal cancer genes identifies potential therapeutic targets. Int. J. Cancer *128*, 1069–1079.

Guardavaccaro, D., Frescas, D., Dorrello, N.V., Peschiaroli, A., Multani, A.S., Cardozo, T., Lasorella, A., Iavarone, A., Chang, S., Hernando, E., and Pagano, M. (2008). Control of chromosome stability by the beta-TrCP-REST-Mad2 axis. Nature *452*, 365–369.

Håkansson, P., Hofer, A., and Thelander, L. (2006). Regulation of mammalian ribonucleotide reduction and dNTP pools after DNA damage and in resting cells. J. Biol. Chem. *281*, 7834–7841.

Hu, C.M., and Chang, Z.F. (2007). Mitotic control of dTTP pool: a necessity or coincidence? J. Biomed. Sci. *14*, 491–497.

Jin, J., Cardozo, T., Lovering, R.C., Elledge, S.J., Pagano, M., and Harper, J.W. (2004). Systematic analysis and nomenclature of mammalian F-box proteins. Genes Dev. *18*, 2573–2580.

Jones, R.J., Baladandayuthapani, V., Neelapu, S., Fayad, L.E., Romaguera, J.E., Wang, M., Sharma, R., Yang, D., and Orlowski, R.Z. (2011). HDM-2 inhibition suppresses expression of ribonucleotide reductase subunit M2, and synergistically enhances gemcitabine-induced cytotoxicity in mantle cell lymphoma. Blood *118*, 4140–4149.

Ke, P.Y., Kuo, Y.Y., Hu, C.M., and Chang, Z.F. (2005). Control of dTTP pool size by anaphase promoting complex/cyclosome is essential for the maintenance of genetic stability. Genes Dev. *19*, 1920–1933.

Kretschmer, C., Sterner-Kock, A., Siedentopf, F., Schoenegg, W., Schlag, P.M., and Kemmner, W. (2011). Identification of early molecular markers for breast cancer. Mol. Cancer *10*, 15.

Kunz, B.A. (1988). Mutagenesis and deoxyribonucleotide pool imbalance. Mutat. Res. *200*, 133–147.

Kunz, B.A., Kohalmi, S.E., Kunkel, T.A., Mathews, C.K., McIntosh, E.M., and Reidy, J.A. (1994). International Commission for Protection Against Environmental Mutagens and Carcinogens. Deoxyribonucleoside triphosphate levels: a critical factor in the maintenance of genetic stability. Mutat. Res. *318*, 1–64.

Kunz, B.A., Ramachandran, K., and Vonarx, E.J. (1998). DNA sequence analysis of spontaneous mutagenesis in Saccharomyces cerevisiae. Genetics *148*, 1491–1505.

Lin, Z.P., Belcourt, M.F., Cory, J.G., and Sartorelli, A.C. (2004). Stable suppression of the R2 subunit of ribonucleotide reductase by R2-targeted short interference RNA sensitizes p53(-/-) HCT-116 colon cancer cells to DNA-damaging agents and ribonucleotide reductase inhibitors. J. Biol. Chem. *279*, 27030–27038.

Lin, Z.P., Belcourt, M.F., Carbone, R., Eaton, J.S., Penketh, P.G., Shadel, G.S., Cory, J.G., and Sartorelli, A.C. (2007). Excess ribonucleotide reductase R2 subunits coordinate the S phase checkpoint to facilitate DNA damage repair and recovery from replication stress. Biochem. Pharmacol. *73*, 760–772.

Lukas, C., Savic, V., Bekker-Jensen, S., Doil, C., Neumann, B., Pedersen, R.S., Grøfte, M., Chan, K.L., Hickson, I.D., Bartek, J., and Lukas, J. (2011). 53BP1 nuclear bodies form around DNA lesions generated by mitotic transmission of chromosomes under replication stress. Nat. Cell Biol. *13*, 243–253.

Martin, L., Rainey, M., Santocanale, C., and Gardner, L.B. (2011). Hypoxic activation of ATR and the suppression of the initiation of DNA replication through cdc6 degradation. Oncogene *2011*, 19.

Mathews, C.K. (2006). DNA precursor metabolism and genomic stability. FASEB J. *20*, 1300–1314.

Mayya, V., Lundgren, D.H., Hwang, S.I., Rezaul, K., Wu, L., Eng, J.K., Rodionov, V., and Han, D.K. (2009). Quantitative phosphoproteomic analysis of T cell receptor signaling reveals system-wide modulation of protein-protein interactions. Sci. Signal. *2*, ra46.

Meraldi, P., Lukas, J., Fry, A.M., Bartek, J., and Nigg, E.A. (1999). Centrosome duplication in mammalian somatic cells requires E2F and Cdk2-cyclin A. Nat. Cell Biol. *1*, 88–93.

Meuth, M. (1989). The molecular basis of mutations induced by deoxyribonucleoside triphosphate pool imbalances in mammalian cells. Exp. Cell Res. *181*, 305–316.

Morikawa, T., Hino, R., Uozaki, H., Maeda, D., Ushiku, T., Shinozaki, A., Sakatani, T., and Fukayama, M. (2010a). Expression of ribonucleotide reductase M2 subunit in gastric cancer and effects of RRM2 inhibition in vitro. Hum. Pathol. *41*, 1742–1748.

Morikawa, T., Maeda, D., Kume, H., Homma, Y., and Fukayama, M. (2010b). Ribonucleotide reductase M2 subunit is a novel diagnostic marker and a potential therapeutic target in bladder cancer. Histopathology *57*, 885–892.

Niida, H., Katsuno, Y., Sengoku, M., Shimada, M., Yukawa, M., Ikura, M., Ikura, T., Kohno, K., Shima, H., Suzuki, H., et al. (2010). Essential role of Tip60-dependent recruitment of ribonucleotide reductase at DNA damage sites in DNA repair during G1 phase. Genes Dev. *24*, 333–338.

Nordlund, P., and Reichard, P. (2006). Ribonucleotide reductases. Annu. Rev. Biochem. *75*, 681–706.

Park, J.H., Park, E.J., Lee, H.S., Kim, S.J., Hur, S.K., Imbalzano, A.N., and Kwon, J. (2006). Mammalian SWI/SNF complexes facilitate DNA double-strand break repair by promoting gamma-H2AX induction. EMBO J. *25*, 3986–3997.

Petroski, M.D., and Deshaies, R.J. (2005). Function and regulation of cullin-RING ubiquitin ligases. Nat. Rev. Mol. Cell Biol. *6*, 9–20.

Phear, G., and Meuth, M. (1989). The genetic consequences of DNA precursor pool imbalance: sequence analysis of mutations induced by excess thymidine at the hamster aprt locus. Mutat. Res. *214*, 201–206.

Reichard, P. (1988). Interactions between deoxyribonucleotide and DNA synthesis. Annu. Rev. Biochem. *57*, 349–374.

Satow, R., Shitashige, M., Kanai, Y., Takeshita, F., Ojima, H., Jigami, T., Honda, K., Kosuge, T., Ochiya, T., Hirohashi, S., and Yamada, T. (2010). Combined functional genome survey of therapeutic targets for hepatocellular carcinoma. Clin. Cancer Res. *16*, 2518–2528.

Schulman, B.A., Lindstrom, D.L., and Harlow, E. (1998). Substrate recruitment to cyclin-dependent kinase 2 by a multipurpose docking site on cyclin A. Proc. Natl. Acad. Sci. USA *95*, 10453–10458.

Shao, J., Zhou, B., Chu, B., and Yen, Y. (2006). Ribonucleotide reductase inhibitors and future drug design. Curr. Cancer Drug Targets *6*, 409–431.

Sherman, P.A., and Fyfe, J.A. (1989). Enzymatic assay for deoxyribonucleoside triphosphates using synthetic oligonucleotides as template primers. Anal. Biochem. *180*, 222–226.

Skaar, J.R., D'Angiolella, V., Pagan, J.K., and Pagano, M. (2009). SnapShot: F Box Proteins II. Cell *137*, 1358.e1–1358.e2.

Tanaka, H., Arakawa, H., Yamaguchi, T., Shiraishi, K., Fukuda, S., Matsui, K., Takei, Y., and Nakamura, Y. (2000). A ribonucleotide reductase gene involved in a p53-dependent cell-cycle checkpoint for DNA damage. Nature *404*, 42–49.

Tetzlaff, M.T., Bai, C., Finegold, M., Wilson, J., Harper, J.W., Mahon, K.A., and Elledge, S.J. (2004). Cyclin F disruption compromises placental development and affects normal cell cycle execution. Mol. Cell. Biol. *24*, 2487–2498.

Wang, X., Liu, X., Xue, L., Zhang, K., Kuo, M.L., Hu, S., Zhou, B., Ann, D., Zhang, S., and Yen, Y. (2011). Ribonucleotide reductase subunit p53R2 regulates mitochondria homeostasis and function in KB and PC-3 cancer cells. Biochem. Biophys. Res. Commun. *410*, 102–107.

Xu, X., Page, J.L., Surtees, J.A., Liu, H., Lagedrost, S., Lu, Y., Bronson, R., Alani, E., Nikitin, A.Y., and Weiss, R.S. (2008). Broad overexpression of ribonucleotide reductase genes in mice specifically induces lung neoplasms. Cancer Res. *68*, 2652–2660.

Xue, L., Zhou, B., Liu, X., Qiu, W., Jin, Z., and Yen, Y. (2003). Wild-type p53 regulates human ribonucleotide reductase by protein-protein interaction with p53R2 as well as hRRM2 subunits. Cancer Res. *63*, 980–986.

Zhang, Y.W., Jones, T.L., Martin, S.E., Caplen, N.J., and Pommier, Y. (2009). Implication of checkpoint kinase-dependent up-regulation of ribonucleotide reductase R2 in DNA damage response. J. Biol. Chem. *284*, 18085–18095.